Curvature elasticity and multi-sphere morphologies

Reinhard Lipowsky

Department of Theory and Bio-Systems, Max Planck Institute of Colloids and Interfaces, Science Park Golm, 14424 Potsdam, Germany

Status. Lipid-protein bilayers form GUVs that attain a fascinating variety of different shapes including many distinct multi-sphere morphologies as predicted by the theory of curvature elasticity [97]. A particularly simple example is provided by budding, i.e. by the formation of a small spherical bud that is still connected to the mother vesicle via a closed membrane neck and points towards the exterior solution as in figure 16(a1) or towards the interior solution as in figure 16(d1) [98]. In these examples, the vesicle membrane was taken to be uniform in composition which implies that it has uniform curvature-elastic properties as well. Budding processes can also be induced by intramembrane domains as in figures 16(a2) and (d2). Such domains arise from lipid phase separation or from the assembly of protein coats [99], and the resulting budding processes represent essential steps for endo- and exocytosis as well as for cytokinesis during cell division.

In addition to shapes with a single bud, the vesicle can also form shapes with several buds as depicted in figures 16(b1) and (e1) for a uniform membrane and in figures 16(b2) and (e2) for a membrane with two types of domains. Furthermore, necklace-like tubes consisting of several spherical beads connected by membrane necks are also possible, see figures 16(c1), (f1) and (c2), (f2) for uniform and multi-domain membranes, respectively. In the following, buds, which are directly connected to the mother vesicle, and beads, which are connected to buds or other beads, will be collectively called spherules.

From the theoretical point of view, the multi-sphere shapes in figures 16(a1)–(f1) are primarily determined by three parameters: membrane area, vesicle volume, and preferred or spontaneous curvature m [98]. In the absence of flip-flops between the two membrane leaflets, the spontaneous curvature contains a nonlocal contribution arising from area-difference-elasticity [100]. Here, I will assume that the membrane contains (at least) one molecular component such as cholesterol that undergoes frequent flip-flops and will, thus, ignore area-difference-elasticity. In the latter case, the spherules have zero bending energy when their radius is equal to $1/|\mathrm{m}|$, i.e. to the absolute value of the inverse spontaneous curvature. In general, we can distinguish two special classes of multi-sphere shapes: shapes with zero-energy spherules and limit shapes obtained via the closure of open necks. For positive spontaneous curvature, another type of limit shape can be formed consisting of spherules that have the same size as the mother vesicle. The latter case includes linear and branched necklace-like tubes.

The spontaneous curvature can vary over several orders of magnitude, from the inverse radius of the GUV to about 1/(10 nm) [38], which implies that the size of the zero-energy spherules can vary over the same range. All multi-sphere shapes displayed in figure 16 are stable for certain parameter regimes, which can be determined by examining the stability of the individual spheres and of the membrane necks [97].

Current and future challenges. Some of the shapes in figure 16 have been observed experimentally but these observations have remained fairly accidental. There are several reasons for this state-of-the-art. First of all, no serious experimental attempts have been made, so far, to control all three shape parameters—area, volume, and spontaneous curvature—simultaneously. Indeed, the standard preparation methods based on lipid film hydration and electroformation produce very polydisperse GUVs with a wide range of sizes. In addition, even though we now have a variety of methods to deduce the value of the spontaneous curvature from budded or tubulated morphologies [37, 38, 101], no reference system is currently available for which the spontaneous curvature can be varied in a systematic and controlled manner.

However, the presumably largest challenge for the preparation and observation of multi-sphere vesicles with a certain architecture is the complexity or 'ruggedness' of the energy landscape associated with curvature elasticity. Some insight into this landscape can be obtained by a gedankenexperiment in which we produce multi-sphere shapes with an increasing number of spherules by osmotic deflation. To be specific, let us consider a membrane with negative spontaneous curvature $\mathrm{m} < 0$ that forms an initially spherical vesicle with volume $V_0 = \frac{4\pi}{3}\mathrm{R}_{\mathrm{ve}}^3$ where the overall vesicle size $\mathrm{R}_{\mathrm{ve}} = \sqrt{\mathrm{A}/(4\pi)}$ is defined in terms of the membrane area A. After deflation, such a vesicle can form a variable number N of (meta)stable in-spherules with radius R_{s}. The latter radius is somewhat variable but is always of the order of $1/|\mathrm{m}|$. It is thus convenient to parametrize the spherule radius as $\mathrm{R}_{\mathrm{s}} = \alpha/|\mathrm{m}|$ with a dimensionless coefficient α. For $\alpha = 1$, the spherules have zero bending energy and are always stable. Deflation of a multi-sphere shape with N zero-energy spherules increases the spherule radius R_{s} until we reach $\mathrm{R}_{\mathrm{s}} = \alpha_*/|\mathrm{m}|$ with $3/2 < \alpha_* \leqslant 3$ as follows from the combined Euler–Lagrange equations for the spherules and the mother vesicle. At this point, the in-spherules become unstable and undergo a sphere-prolate (SP) bifurcation. The precise value of α_* depends on the radius R_{l} of the mother vesicle and reaches the limiting value $\alpha_* = 3$ for large R_{l}.

A vesicle with N in-spherules of radius $\mathrm{R}_{\mathrm{s}} = \alpha/|\mathrm{m}|$ has the volume

$$\mathrm{V}(\mathrm{N},\alpha) = \mathrm{V}_0\left(\left[1-\mathrm{N}\left(\frac{\alpha}{|\mathrm{m}|\,\mathrm{R}_{\mathrm{ve}}}\right)^2\right]^{3/2} - \mathrm{N}\left(\frac{\alpha}{|\mathrm{m}|\,\mathrm{R}_{\mathrm{ve}}}\right)^3\right). \tag{3}$$

It is important to note, however, that a vesicle with volume $\mathrm{V}(\mathrm{N},\alpha)$ can attain, for fixed values of $\mathrm{N} > 1$ and α, several multi-sphere morphologies as depicted in figures 17(a)–(d) for $3 \leqslant \mathrm{N} \leqslant 6$. Because the spherule radius can vary over a certain range, a vesicle with volume $\mathrm{V}(\mathrm{N},\alpha)$ can also form alternative morphologies with less than N spherules and a spherule radius that exceeds $\alpha/|\mathrm{m}|$.

Inspection of figure 17 reveals that we can obtain, for each N, a certain number $|\Omega|$ of distinct morphologies. This number

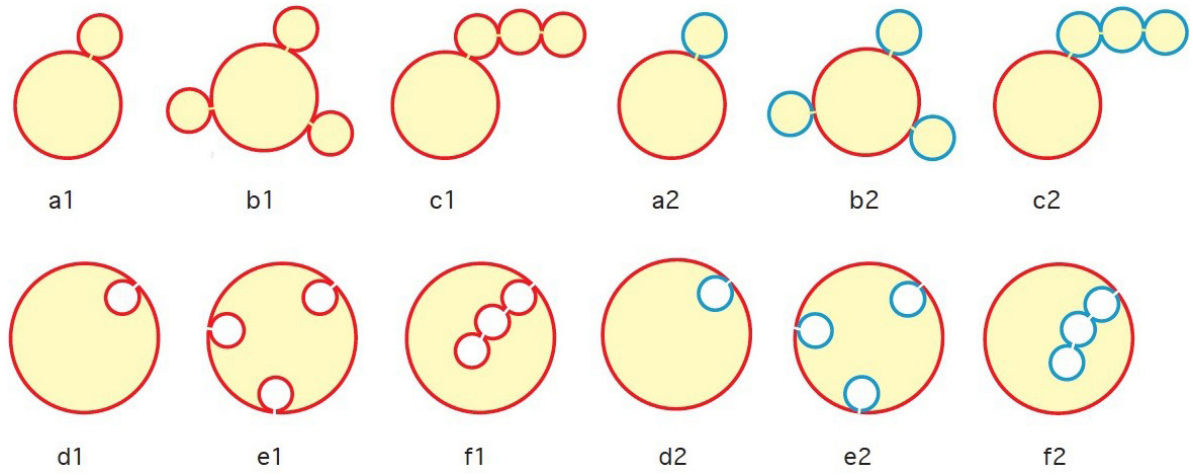

Figure 16. Multi-sphere shapes consisting of a spherical mother vesicle to which spherules, corresponding to small spherical buds and beads, are connected via closed membrane necks. The interior aqueous solution is yellow, the exterior one is white: (a1)–(c1) uniform membranes (red) with positive spontaneous curvature form out-buds and necklace-like tubes pointing towards the exterior solution; (d1)–(f1) uniform membranes (red) with negative spontaneous curvature form in-buds and necklace-like tubes pointing towards the interior solution; (a2)–(c2) membranes with two types of intramembrane domains (red, blue) and positive spontaneous curvature; and (d2)–(f2) multi-domain membranes (red, blue) with negative spontaneous curvature.

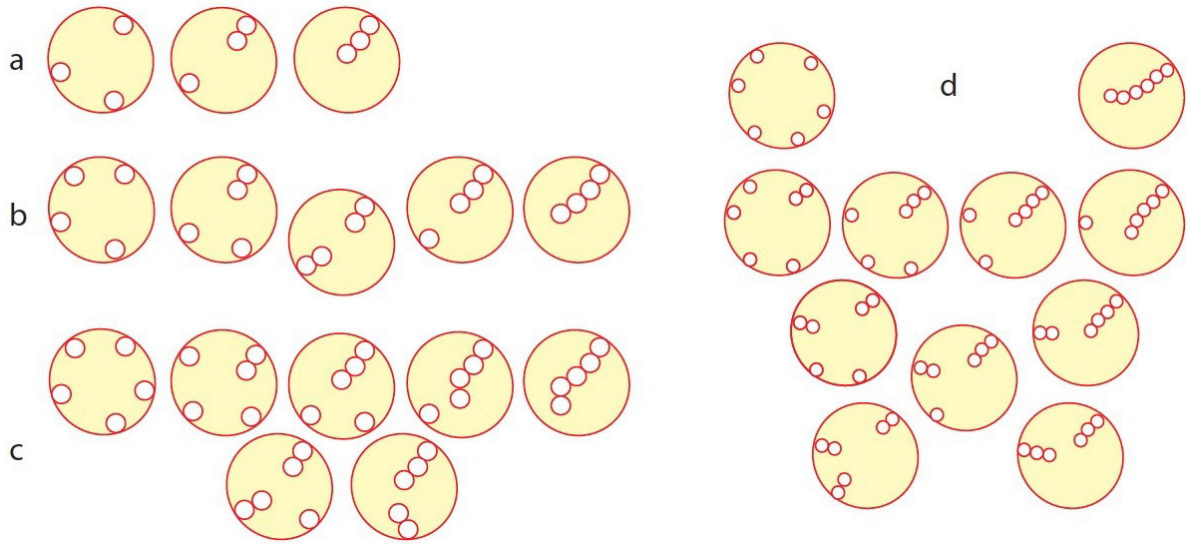

Figure 17. Morphological complexity emerging from multi-sphere vesicles with N spherules for negative spontaneous curvature $m < 0$: (a) three morphologies with $N = 3$; (b) five morphologies with $N = 4$; (c) seven morphologies with $N = 5$; and (d) eleven morphologies with $N = 6$. For given membrane area, vesicle volume, and spontaneous curvature, all morphologies with the same spherule number N have the same spherule radius R_s and the same curvature energy. The spherule radius R_s can vary between $R_s = 1/|m|$ and $R_s = \alpha_*/|m|$ with $\alpha_* < 3$, see main text. For visual simplicity, all necklaces and buds have been placed into the plane of the figure, and the membrane necks connecting different spherical segments have been omitted.

increases from $|\Omega| = 3$ for $N = 3$ to $|\Omega| = 11$ for $N = 6$. In fact, for large values of N, the number $|\Omega|$ increases exponentially with $\sqrt{N}$. Furthermore, for a given membrane area, vesicle volume, and spontaneous curvature, multi-sphere morphologies with the same spherule number N have the same spherule radius R_s and the same curvature energy.

The morphologies depicted in figure 17 can be obtained via two basic shape transformations [37], the nucleation of a new bud via an oblate-stomatocyte (OS) bifurcation and the addition of a new bead to an existing bud or necklace via the afore-mentioned SP bifurcation. Both types of bifurcation are discontinuous and exhibit hysteresis. The OS bifurcation leads to (meta)stable spherules with radius $R_s = \alpha/|m|$ and $1/(2+\varepsilon) \leqslant \alpha < 3$ where the lower bound for α depends on the radius R_l of the mother vesicle via the small correction term $\varepsilon = 1/(|m| R_l) \ll 1$ as follows from the neck closure condition. Furthermore, starting from any N-spherule morphology, we can generate several distinct $(N+1)$-spherule morphologies by either nucleating a new bud or extending an existing bud or necklace. In this way, we can generate the different morphologies by different sequences of OS and SP bifurcations which implies a rather rugged energy landscape. Likewise, when the closed necks of the different N-spherule morphologies are opened up by changes in vesicle volume or spontaneous

curvature, we will obtain quite different vesicle shapes which again reveals that each of the $|\Omega|$ distinct morphologies with N in-spherules belongs to a different energy branch.

Repeating the osmotic deflation towards a certain volume $V = V(N, \alpha)$ several times, we will typically find different outcomes for the morphologies. When we reduce the vesicle volume to $V = V(4, 1)$, for example, we can obtain any of the multi-sphere morphologies depicted in figures 17(a) and (b) as well as intermediate morphologies with open necks. Therefore, when we perform such a deflation step many times, for the same initial volume V_0 and the same spontaneous curvature $m < 0$, we expect to obtain a certain probability distribution $P(S_j|V)$ for the accessible multi-sphere shapes S_j. This probability distribution reflects the underlying energy landscape and introduces a probabilistic aspect into the morphology of vesicles.

Advances in science and technology to meet challenges, concluding remarks. Recently, it has become possible to produce large populations of monodisperse GUVs using microfluidic double emulsions [102, 103] or pico-injection of small vesicles into emulsion droplets [104]. Furthermore, it now seems feasible to develop membrane systems for which the spontaneous curvature can be controlled in a systematic manner. Combining both developments, we should be able to produce monodisperse batches of vesicles with the same spontaneous curvature. Subsequent deflation can then produce many multi-sphere morphologies with the same volume $V(N, \alpha)$ as in (3). In this way, it should become possible to actually measure the statistics of the N-spherule morphologies and, thus, the probability distribution $P(S_j|V)$. Finally, it would be rather valuable to develop methods by which we can open and close the necks of multi-sphere shapes in a reversible and controlled manner. We could then develop storage and delivery systems based on these shapes.

Acknowledgments

I thank Rumiana Dimova for the opportunity to participate in this Roadmap and the MaxSynBio consortium, jointly funded by the Max Planck Gesellschaft and the Federal Ministry of Research, Germany, for a stimulating scientific environment.

Reinhard Lipowsky https://orcid.org/0000-0001-8417-8567
Thomas J Pucadyil https://orcid.org/0000-0002-2907-9889
Wade F Zeno https://orcid.org/0000-0002-2341-8923
Jeanne C Stachowiak https://orcid.org/0000-0003-2501-142X
Dimitrios Stamou https://orcid.org/0000-0001-8456-8995
Artù Breuer https://orcid.org/0000-0001-9831-1103
Line Lauritsen https://orcid.org/0000-0002-6378-571X
Camille Simon https://orcid.org/0000-0002-7060-5721
Cécile Sykes https://orcid.org/0000-0003-3057-2600
Gregory A Voth https://orcid.org/0000-0002-3267-6748
Thomas R Weikl https://orcid.org/0000-0002-0911-5328

References

[1] Simunovic M, Voth G A, Callan-Jones A and Bassereau P 2015 When physics takes over: BAR proteins and membrane curvature *Trends Cell Biol.* **25** 780–92
[2] Peter B J, Kent H M, Mills I G, Vallis Y, Butler P J G, Evans P R and McMahon H T 2004 BAR domains as sensors of membrane curvature: the amphiphysin BAR structure *Science* **303** 495–9
[3] Callan-Jones A and Bassereau P 2013 Curvature-driven membrane lipid and protein distribution *Curr. Opin. Solid State Mater. Sci.* **17** 143–50
[4] Johannes L, Wunder C and Bassereau P 2014 Bending 'on the rocks'—a cocktail of biophysical modules to build endocytic pathways *Cold Spring Harb. Perspect. Biol.* **6** a016741
[5] Shi Z and Baumgart T 2014 Dynamics and instabilities of lipid bilayer membrane shapes *Adv. Colloid Interface Sci.* **208** 76–88
[6] Simunovic M, Evergren E, Golushko I, Prévost C, Renard H-F, Johannes L, McMahon H, Lorman V, Voth G A and Bassereau P 2016 How curvature-generating proteins build scaffolds on membrane nanotubes *Proc. Natl Acad. Sci. USA* **113** 11226–31
[7] Frost A, Perera R, Roux A, Spasov K, Destaing O, Egelman E H, De Camilli P and Unger V M 2008 Structural basis of membrane invagination by F-BAR domains *Cell* **132** 807–17
[8] Prevost C, Zhao H, Manzi J, Lemichez E, Lappalainen P, Callan-Jones A and Bassereau P 2015 IRSp53 senses negative membrane curvature and phase separates along membrane tubules *Nat. Commun.* **6** 8529
[9] Simunovic M *et al* 2017 Friction mediates scission of tubular membranes scaffolded by BAR proteins *Cell* **170** 172–84
[10] Noguchi H 2016 Membrane tubule formation by banana-shaped proteins with or without transient network structure *Sci. Rep.* **6** 20935
[11] Dar S, Kamerkar S C and Pucadyil T J 2015 A high-throughput platform for real-time analysis of membrane fission reactions reveals dynamin function *Nat. Cell Biol.* **17** 1588–96
[12] Bhatia V K, Madsen K L, Bolinger P-Y, Kunding A, Hedegard P, Gether U and Stamou D 2009 Amphipathic motifs in BAR domains are essential for membrane curvature sensing *EMBO J.* **28** 3303–14
[13] Segrest J P, Deloof H, Dohlman J G, Brouillette C G and Anantharamaiah G M 1990 Amphipathic helix motif—classes and properties *Proteins* **8** 103–17
[14] Schmidt N W and Wong G C L 2013 Antimicrobial peptides and induced membrane curvature: Geometry, coordination chemistry, and molecular engineering *Curr. Opin. Solid State Mater. Sci.* **17** 151–63
[15] Drin G and Antonny B 2010 Amphipathic helices and membrane curvature *FEBS Lett.* **584** 1840–7
[16] Simunovic M, Prevost C, Callan-Jones A and Bassereau P 2016 Physical basis of some membrane shaping mechanisms *Phil. Trans. R. Soc.* A **374** 2016
[17] Jao C C, Hegde B G, Chen J, Haworth I S and Langen R 2008 Structure of membrane-bound alpha-synuclein from site-directed spin labeling and computational refinement *Proc. Natl Acad. Sci. USA* **105** 19666–71
[18] Hohlweg W, Kosol S and Zangger K 2012 Determining the orientation and localization of membrane-bound peptides *Curr. Protein Peptide Sci.* **13** 267–79
[19] Tenchov B G, MacDonald R C and Lentz B R 2013 Fusion peptides promote formation of bilayer cubic phases in lipid dispersions. An x-ray diffraction study *Biophys. J.* **104** 1029–37
[20] Campelo F, McMahon H T and Kozlov M M 2008 The hydrophobic insertion mechanism of membrane curvature generation by proteins *Biophys. J.* **95** 2325–39
[21] Harries D, Ben-Shaul A and Szleifeo I 2004 Enveloping of charged proteins by lipid bilayers *J. Phys. Chem.* B **108** 1491–6
[22] Strandberg E, Zerweck J, Wadhwani P and Ulrich A S 2013 Synergistic insertion of antimicrobial magainin-family peptides in membranes depends on the lipid spontaneous curvature *Biophys. J.* **104** L9–11
[23] Lemkul J A, Huang J, Roux B and MacKerell A D 2016 An empirical polarizable force field based on the classical drude oscillator model: development history and recent applications *Chem. Rev.* **116** 4983–5013
[24] Perrin B S, Sodt A J, Cotten M L and Pastor R W 2015 The curvature induction of surface-bound antimicrobial peptides piscidin 1 and piscidin 3 varies with lipid chain length *J. Membr. Biol.* **248** 455–67
[25] Deserno M 2015 Fluid lipid membranes: from differential geometry to curvature stresses *Chem. Phys. Lipids* **185** 11
[26] Kozlovsky Y and Kozlov M M 2002 Stalk model of membrane fusion: solution of energy crisis *Biophys. J.* **82** 882
[27] Hu M, Briguglio J J and Deserno M 2012 Determining the Gaussian curvature modulus of lipid membranes in simulations *Biophys. J.* **102** 1403
[28] Helfrich W 1981 Amphiphilic mesophases made of defects *Physics of Defects* (North Holland: Amsterdam)
[29] Hamm M and Kozlov M M 2000 Elastic energy of tilt and bending of fluid membranes *Eur. Phys. J.* E **3** 323
[30] Hu M, de Jong D H, Marrink S J and Deserno M 2013 Gaussian curvature elasticity determined from global shape transformations and local stress distributions: a comparative study using the MARTINI model *Farad. Discuss.* **161** 365
[31] Venable R M, Brown F L H and Pastor R W 2015 Mechanical properties of lipid bilayers from molecular dynamics simulation *Chem. Phys. Lipids* **192** 60
[32] Imparato A, Shillcock J C and Lipowsky R 2005 Shape fluctuations and elastic properties of two-component bilayer membranes *Europhys. Lett.* **69** 650
[33] Sodt A J, Venable R M, Lyman E and Pastor R W 2016 Nonadditive compositional curvature energetics of lipid bilayers *Phys. Rev. Lett.* **117** 138104
[34] Terzi M M and Deserno M 2017 Novel tilt-curvature coupling in lipid membranes *J. Chem. Phys.* **147** 084702
[35] Liu Y and Nagle J F 2004 Diffuse scattering provides material parameters and electron density profiles of biomembranes *Phys. Rev.* E **69** 040901
[36] Fadeel B and Xue D 2009 The ins and outs of phospholipid asymmetry in the plasma membrane: roles in health and disease *Crit. Rev. Biochem. Mol. Biol.* **44** 264–77
[37] Liu Y G, Agudo-Canalejo J, Grafmuller A, Dimova R and Lipowsky R 2016 Patterns of flexible nanotubes formed by

liquid-ordered and liquid-disordered membranes *ACS Nano* **10** 463–74
[38] Lipowsky R 2013 Spontaneous tubulation of membranes and vesicles reveals membrane tension generated by spontaneous curvature *Faraday Discuss.* **161** 305–31
[39] Dasgupta R, Miettinen M, Fricke N, Lipowsky R and Dimova R 2018 The glycolipid GM1 reshapes asymmetric biomembranes and giant vesicles by curvature generation *Proc. Natl Acad. Sci. USA* **115** 5756–61
[40] Dimova R, Aranda S, Bezlyepkina N, Nikolov V, Riske K A and Lipowsky R 2006 A practical guide to giant vesicles. Probing the membrane nanoregime via optical microscopy *J. Phys.: Condens. Matter* **18** S1151–76
[41] Dobereiner H G, Selchow O and Lipowsky R 1999 Spontaneous curvature of fluid vesicles induced by trans-bilayer sugar asymmetry *Eur. Biophys. J.* **28** 174–8
[42] Nikolov V, Lipowsky R and Dimova R 2007 Behavior of giant vesicles with anchored DNA molecules *Biophys. J.* **92** 4356–68
[43] McMahon H T and Gallop J L 2005 Membrane curvature and mechanisms of dynamic cell membrane remodelling *Nature* **438** 590–6
[44] Simunovic M, Lee K Y C and Bassereau P 2015 Celebrating soft matter's 10th anniversary: screening of the calcium-induced spontaneous curvature of lipid membranes *Soft Matter* **11** 5030–6
[45] Graber Z T, Shi Z and Baumgart T 2017 Cations induce shape remodeling of negatively charged phospholipid membranes *Phys. Chem. Chem. Phys.* **19** 15285–95
[46] Sorre B, Callan-Jones A, Manzi J, Goud B, Prost J, Bassereau P and Roux A 2012 Nature of curvature coupling of amphiphysin with membranes depends on its bound density *Proc. Natl Acad. Sci. USA* **109** 173–8
[47] Steinkühler J, De Tillieux P, Knorr R L, Lipowsky R and Dimova R 2018 Charged giant unilamellar vesicles prepared by electroformation exhibit nanotubes and transbilayer lipid asymmetry *Sci. Rev.* in revision
[48] Mattila J P *et al* 2015 A hemi-fission intermediate links two mechanistically distinct stages of membrane fission. *Nature* **524** 109–13
[49] Bashkirov P V *et al* 2008 GTPase cycle of dynamin is coupled to membrane squeeze and release, leading to spontaneous fission *Cell* **135** 1276–86
[50] Shnyrova A V *et al* 2013 Geometric catalysis of membrane fission driven by flexible dynamin rings *Science* **339** 1433–6
[51] Praefcke G J and McMahon H T 2004 The dynamin superfamily: universal membrane tubulation and fission molecules? *Nat. Rev.* **5** 133–47
[52] Ferguson S M and De Camilli P 2012 Dynamin, a membrane-remodelling GTPase *Nat. Rev.* **13** 75–88
[53] Schmid S L and Frolov V A 2011 Dynamin: functional design of a membrane fission catalyst *Annu. Rev. Cell Dev. Biol.* **27** 79–105
[54] Antonny B *et al* 2016 Membrane fission by dynamin: what we know and what we need to know *EMBO J.* **35** 2270–84
[55] Pucadyil T J and Schmid S L 2009 Conserved functions of membrane active GTPases in coated vesicle formation *Science* **325** 1217–20
[56] Dar S and Pucadyil T J 2017 The pleckstrin-homology domain of dynamin is dispensable for membrane constriction and fission *Mol. Biol. Cell* **28** 152–60
[57] Snead W T *et al* 2017 Membrane fission by protein crowding *Proc. Natl Acad. Sci. USA* **114** E3258–67
[58] Frolov V A, Escalada A, Akimov S A and Shnyrova A V 2015 Geometry of membrane fission *Chem. Phys. Lipids* **185** 129–40
[59] Evans E, Heinrich V, Ludwig F and Rawicz W 2003 Dynamic tension spectroscopy and strength of biomembranes *Biophys. J.* **85** 2342–50
[60] Zhang G and Muller M 2017 Rupturing the hemi-fission intermediate in membrane fission under tension: reaction coordinates, kinetic pathways, and free-energy barriers *J. Chem. Phys.* **147** 064906
[61] Chiaruttini N *et al* 2015 Relaxation of loaded ESCRT-III spiral springs drives membrane deformation *Cell* **163** 866–79
[62] Imig C, Min S W, Krinner S, Arancillo M, Rosenmund C, Südhof T C, Rhee J, Brose N and Cooper B H 2014 The morphological and molecular nature of synaptic vesicle priming at presynaptic active zones *Neuron* **84** 416–31
[63] Zhou Q, Zhou P, Wang A L, Wu D, Zhao M, Südhof T C and Brunger A T 2017 The primed SNARE-complexin-synaptotagmin complex for neuronal exocytosis *Nature* **548** 420–5
[64] Xu J *et al* 2017 Mechanistic insights into neurotransmitter release and presynaptic plasticity from the crystal structure of Munc13-1 C1C2BMUN *Elife* **6** e22567
[65] D'Agostino M, Risselada H J, Lürick A, Ungermann C and Mayer A 2017 A tethering complex drives the terminal stage of SNARE-dependent membrane fusion *Nature* **551** 634–8
[66] Bharat T A, Malsam J, Hagen W J, Scheutzow A, Söllner T H and Briggs J A 2014 SNARE and regulatory proteins induce local membrane protrusions to prime docked vesicles for fast calcium-triggered fusion *EMBO Rep.* **15** 308–14
[67] Hernandez J M, Stein A, Behrmann E, Riedel D, Cypionka A, Farsi Z, Walla P J, Raunser S and Jahn R 2012 Membrane fusion intermediates via directional and full assembly of the SNARE complex *Science* **336** 1581–4
[68] Hishida M, Nomura Y, Akiyama R, Yamamura Y and Saito K 2017 Electrostatic double-layer interaction between stacked charged bilayers *Phys. Rev.* E **96** 040601
[69] Aeffner S, Reusch T, Weinhausen B and Saldit T 2012 Energetics of stalk intermediates in membrane fusion are controlled by lipid composition *Proc. Natl. Acad. Sci. USA* **109** 1609–18
[70] Komorowski K, Salditt A, Xu Y, Yavuz H, Brennich M, Jahn R and Salditt T 2017 Vesicle adhesion and fusion studied by small-angle x-ray scattering *Biophys. J.* **114** 1908–20
[71] Howes M T *et al* 2010 *J. Cell Biol.* **190** 675
[72] Johannes L, Wunder C and Shafaq-Zadah M 2016 *J. Mol. Biol.* **428** 4792
[73] Römer W 2007 *Nature* **450** 670
[74] Pezeshkian W, Hansen A G, Johannes L, Khandelia H, Shillcock J, Sunil Kumar P B and Ipsen J H 2016 *Soft Matter* **12** 5164
[75] Damm E M, Pelkmans L, Kartenbeck J, Mezzacasa A, Kurzchalia T V and Helenius A 2005 *J. Cell Biol.* **168** 477
[76] Ewers H *et al* 2010 *Nat. Cell Biol.* **12** 11
[77] Pezeshkian W, Gao H, Arumugam S, Becken U, Bassereau P, Florent J C, Ipsen J H, Johannes L and Shillcock J 2017 *ACS Nano* **11** 314
[78] Casimir H B G and Polder D 1948 *Phys. Rev.* **73** 360
[79] Li H and Kardar M 1992 *Phys. Rev.* A **46** 6490
[80] Goulian M, Bruinsma R and Pincus P 1993 *Europhys. Lett.* **22** 145
[81] Lakshminarayan R *et al* 2014 *Nat. Cell Biol.* **16** 595
[82] Canham P B 1970 The minimum energy of bending as a possible explanation of the biconcave shape of the human red blood cell *J. Theor. Biol.* **26** 61–81
[83] Evans E and Skalak R 1980 *Mechanics and Thermodynamics of Biomembranes* (Boca Raton, FL: CRC Press)
[84] Helfrich W 1973 Elastic properties of lipid bilayers: theory and possible experiments *Z. Naturforsch.* **28c** 693–703
[85] Mitov M D 1978 Third and fourth order curvature elasticity of lipid bilayers *C. R. Acad. Bulg. Sci.* **31** 513–5
[86] Kozlov M M and Winterhalter M 1991 Elastic moduli for strongly curved monolayers. Position of the neutral surface *J. Phys.* II **1** 1077–84

[87] Nagle J F 2017 Experimentally determined tilt and bending moduli of single-component lipid bilayers *Chem. Phys. Lipids* **205** 18–24

[88] Lipowsky R 1995 The morphology of lipid membranes *Curr. Opin. Struct. Biol.* **5** 531–40

[89] Kozlov M M, McMahon H T and Chernomordik L V 2010 Protein-driven membrane stresses in fusion and fission *Trends Biochem. Sci.* **35** 699–706

[90] Seddon J M and Templer R H 1995 Polymorphism of lipid-water systems *Structure and Dynamics of Membranes* eds R Lipowsky and E Sackmann (Amsterdam: Elsevier) pp 97–160

[91] Helfrich W 1978 Steric interaction of fluid membranes in multilayer system *Z. Naturforsch.* **33a** 305–15

[92] Yolcu C and Deserno M 2012 Membrane-mediated interactions between rigid inclusions: an effective field theory *Phys. Rev.* E **86** 031906

[93] Shibata Y, Hu J, Kozlov M M and Rapoport T A 2009 Mechanisms shaping the membranes of cellular organelles *Annu. Rev. Cell Dev. Biol.* **25** 329–54

[94] Lee C and Chen L B 1988 Dynamic behavior of endoplasmic-reticulum in living cells *Cell* **54** 37–46

[95] Nixon-Abell J *et al* 2016 Increased spatiotemporal resolution reveals highly dynamic dense tubular matrices in the peripheral ER *Science* **354** aaf3928

[96] Ladinsky M S, Mastronarde D N, McIntosh J R, Howell K E and Staehelin L A 1999 Golgi structure in three dimensions: functional insights from the normal rat kidney cell *J. Cell Biol.* **144** 1135–49

[97] Lipowsky R 2019 Understanding giant vesicles: a theoretical perspective *The Giant Vesicle Book* eds R Dimova and C Marques (London: Taylor and Francis) accepted

[98] Seifert U, Berndl K and Lipowsky R 1991 Shape transformations of vesicles: phase diagram for spontaneous curvature and bilayer coupling model *Phys. Rev.* A **44** 1182–202

[99] Agudo-Canalejo J and Lipowsky R 2015 Critical particle sizes for the engulfment of nanoparticles by membranes and vesicles with bilayer asymmetry *ACS Nano* **9** 3704–20

[100] Döbereiner H-G, Evans E, Kraus M, Seifert U and Wortis M 1997 Mapping vesicle shapes into the phase diagram: a comparison of experiment and theory *Phys. Rev.* E **55** 4458–74

[101] Bhatia T, Agudo-Canalejo J, Dimova R and Lipowsky R 2018 Membrane nanotubes increase the robustness of giant vesicles *ACS Nano* **12** 4478–85

[102] Arriaga L R, Datta S S, Kim S-H, Amstad E, Kodger T E, Monroy F and Weitz D A 2014 Ultrathin shell double emulsion templated giant unilamellar lipid vesicles with controlled microdomain formation *Small* **10** 950–6

[103] Petit J, Polenz I, Baret J-C, Herminghaus S and Baeumchen O 2016 Vesicles-on-a-chip: a universal microfluidic platform for the assembly of liposomes and polymersomes *Eur. Phys. J.* E **39** 1–6

[104] Weiss M *et al* 2018 Sequential bottom-up assembly of mechanically stabilized cell-like proteoliposomes by microfluidics *Nat. Mater.* **17** 89–95

[105] Kozlovsky Y and Kozlov M M 2003 Membrane fission: model for intermediate structures *Biophys. J.* **85** 85–96

[106] Suzuki D T, Grigliatti T and Williamson R 1971 Temperature-sensitive mutations in *Drosophila melanogaster*. VII. A mutation (para^{ts}) causing reversible adult paralysis *Proc. Natl Acad. Sci. USA* **68** 890–3

[107] Hinshaw J E and Schmid S L 1995 Dynamin self-assembles into rings suggesting a mechanism for coated vesicle budding *Nature* **374** 190–2

[108] Sweitzer S M and Hinshaw J E 1998 Dynamin undergoes a GTP-dependent conformational change causing vesiculation *Cell* **93** 1021–9

[109] Roux A, Koster G, Lenz M, Sorre B, Manneville J-B, Nassoy P and Bassereau P 2010 Membrane curvature controls dynamin polymerization *Proc. Natl Acad. Sci. USA* **107** 4141–6

[110] Sundborger A C, Fang S, Heymann J A, Ray P, Chappie J S and Hinshaw J E 2014 A dynamin mutant defines a superconstricted prefission state *Cell Rep.* **8** 734–42

[111] Lipowsky R 1995 Bending of membranes by anchored polymers *Europhys. Lett.* **30** 197–202

[112] Stachowiak J C, Hayden C C and Sasaki D Y 2010 Steric confinement of proteins on lipid membranes can drive curvature and tubulation *Proc. Natl Acad. Sci. USA* **107** 7781–6

[113] Stachowiak J, Schmid E, Ryan C, Ann H, Sasaki D, Sherman M, Geissler P, Fletcher D and Hayden C 2012 Membrane bending by protein–protein crowding *Nat. Cell Biol.* **14** 944

[114] Snead W T, Hayden C C, Gadok A K, Zhao C, Rangamani P, Lafer E M and Stachowiak J C 2017 Membrane fission by protein crowding *Proc. Natl Acad. Sci. USA* **114** E3258–67

[115] Kory N, Thiam A, Farese R and Walther T 2015 Protein crowding is a determinant of lipid droplet protein composition *Dev. Cell* **34** 351–63

[116] Busch D J, Houser J R, Hayden C C, Sherman M B, Lafer E M and Stachowiak J C 2015 Intrinsically disordered proteins drive membrane curvature, *Nat. Commun.* **6** 7875

[117] Bhagatji P, Leventis R, Comeau J, Refaei M and Silvius J R 2009 Steric and not structure-specific factors dictate the endocytic mechanism of glycosylphosphatidylinositol-anchored proteins *J. Cell Biol.* **186** 615–28

[118] Copic A, Latham C, Horlbeck M, D'Arcangelo J and Miller E 2012 Er cargo properties specify a requirement for copii coat rigidity mediated by Sec13p *Science* **335** 1359–62

[119] Chung I, Reichelt M, Shao L, Akita R W, Koeppen H, Rangell L, Schaefer G, Mellman I and Sliwkowski M X 2016 High cell-surface density of HER2 deforms cell membranes *Nat. Commun.* **7** 12742

[120] Soranno A, Koenig I, Borgia M B, Hofmann H, Zosel F, Nettels D and Schuler B 2014 Single-molecule spectroscopy reveals polymer effects of disordered proteins in crowded environments *Proc. Natl Acad. Sci. USA* **111** 4874–9

[121] Zimmerberg J and Kozlov M M 2006 How proteins produce cellular membrane curvature *Nat. Rev. Mol. Cell Biol.* **7** 9–19

[122] Iversen L, Mathiasen S, Larsen J B and Stamou D 2015 Membrane curvature bends the laws of physics and chemistry *Nat. Chem. Biol.* **11** 822–5

[123] Bigay J, Gounon P, Robineau S and Antonny B 2003 Lipid packing sensed by ArfGAP1 couples COPI coat disassembly to membrane bilayer curvature *Nature* **426** 563–6

[124] Callan-Jones A, Sorre B and Bassereau P 2011 Curvature-driven lipid sorting in biomembranes *Cold Spring Harb. Perspect. Biol.* **3** a004648

[125] Larsen J B *et al* 2015 Membrane curvature enables N-Ras lipid anchor sorting to liquid-ordered membrane phases *Nat. Chem. Biol.* **11** 192–4

[126] Rosholm K R *et al* 2017 Membrane curvature regulates ligand-specific membrane sorting of GPCRs in living cells *Nat. Chem. Biol.* **13** 724–9

[127] Tønnesen A, Christensen S M, Tkach V and Stamou D 2014 Geometrical membrane curvature as an allosteric regulator of membrane protein structure and function *Biophys. J.* **106** 201–9

[128] Baumgart T, Capraro B R, Zhu C and Das S L 2011 Thermodynamics and mechanics of membrane curvature generation and sensing by proteins and lipids *Annu. Rev. Phys. Chem.* **62** 483–506

[129] Zhao W *et al* 2017 Nanoscale manipulation of membrane curvature for probing endocytosis in live cells *Nat. Nanotechnol.* **12** 750–6
[130] Elliott H, Fischer R S, Myers K A, Desai R A, Gao L, Chen C S, Adelstein R S, Waterman C M and Danuser G 2015 Myosin II controls cellular branching morphogenesis and migration in three dimensions by minimizing cell-surface curvature *Nat. Cell Biol.* **17** 137–47
[131] Alberts B, Johnson A, Lewis J, Raff M, Roberts K and Walte P 2002 *Molecular Biology of the Cell* 4th edn (New York: Garland Science)
[132] Kukulski W, Schorb M, Kaksonen M and Briggs J A 2012 Plasma membrane reshaping during endocytosis is revealed by time-resolved electron tomography *Cell* **150** 508–20
[133] Boulant S, Kural C, Zeeh J C, Ubelmann F and Kirchhausen T 2011 Actin dynamics counteract membrane tension during clathrin-mediated endocytosis *Nat. Cell Biol.* **13** 1124–31
[134] Idrissi F Z, Blasco A, Espinal A and Geli M I 2012 Ultrastructural dynamics of proteins involved in endocytic budding *Proc. Natl Acad. Sci. USA* **109** E2587–94
[135] Rodal A A, Manning A L, Goode B L and Drubin D G 2003 Negative regulation of yeast WASp by two SH3 domain-containing proteins *Curr. Biol.* **13** 1000–8
[136] Berro J and Pollard T D 2014 Synergies between Aip1p and capping protein subunits (Acp1p and Acp2p) in clathrin-mediated endocytosis and cell polarization in fission yeast *Mol. Biol. Cell* **25** 3515–27
[137] Sykes C and Plastino J 2010 Cell biology: actin filaments up against a wall *Nature* **464** 365–6
[138] Picco A, Kukulski W, Manenschijn H E, Specht T, Briggs J A G and Kaksonen M 2018 The contributions of the actin machinery to endocytic membrane bending and vesicle formation *Mol. Biol. Cell* **29** 1346–58
[139] Boukellal H, Campas O, Joanny J-F, Prost J and Sykes C 2004 Soft listeria: actin-based propulsion of liquid drops *Phys. Rev.* E **69** 061906
[140] Carvalho K, Lemiere J, Faqir F, Manzi J, Blanchoin L, Plastino J, Betz T and Sykes C 2013 Actin polymerization or myosin contraction: two ways to build up cortical tension for symmetry breaking *Phil. Trans. R. Soc.* B **368** 20130005
[141] Simunovic M, Mim C, Marlovits T C, Resch G, Unger V M and Voth G A 2013 Protein-mediated transformation of lipid vesicles into tubular networks *Biophys. J.* **105** 711–9
[142] Simunovic M, Srivastava A and Voth G A 2013 Linear aggregation of proteins on the membrane as a prelude to membrane remodeling *Proc. Natl Acad. Sci. USA* **110** 20396–401
[143] Simunovic M and Voth G A 2015 Membrane tension controls the assembly of curvature-generating proteins *Nat. Commun.* **6** 7219
[144] Cui H, Lyman E and Voth G A 2011 Mechanism of membrane curvature sensing by amphipathic helix containing proteins *Biophys. J.* **100** 1271–9
[145] Chen Z, Zhu C, Kuo C J, Robustelli J and Baumgart T 2016 The N-terminal amphipathic helix of endophilin does not contribute to its molecular curvature generation capacity *J. Am. Chem. Soc.* **138** 14616–22
[146] Chen Z, Atefi E and Baumgart T 2016 Membrane shape instability induced by protein crowding *Biophys. J.* **111** 1823–6
[147] Meinecke M, Boucrot E, Camdere G, Hon W C, Mittal R and McMahon H T 2013 Cooperative recruitment of dynamin and BIN/amphiphysin/Rvs (BAR) domain-containing proteins leads to GTP-dependent membrane scission *J. Biol. Chem.* **288** 6651–61
[148] Sundborger A, Soderblom C, Vorontsova O, Evergren E, Hinshaw J E and Shupliakov O 2011 An endophilin-dynamin complex promotes budding of clathrin-coated vesicles during synaptic vesicle recycling *J. Cell Sci.* **124** 133–43
[149] Takeda T *et al* 2018 Dynamic clustering of dynamin-amphiphysin helices regulates membrane constriction and fission coupled with GTP hydrolysis *Elife* **7** e30246
[150] Takei K, Slepnev V I, Haucke V and De Camilli P 1999 Functional partnership between amphiphysin and dynamin in clathrin-mediated endocytosis *Nat. Cell Biol.* **1** 33–9
[151] Bahrami A H, Lipowsky R and Weikl T R 2012 Tubulation and aggregation of spherical nanoparticles adsorbed on vesicles *Phys. Rev. Lett.* **109** 188102
[152] van der Wel C, Vahid A, Saric A, Idema T, Heinrich D and Kraft D J 2016 Lipid membrane-mediated attraction between curvature inducing objects *Sci. Rep.* **6** 32825
[153] Raatz M, Lipowsky R and Weikl T R 2014 Cooperative wrapping of nanoparticles by membrane tubes *Soft Matter* **10** 3570
[154] Raatz M and Weikl T R 2017 Membrane tubulation by elongated and patchy nanoparticles *Adv. Mater. Interfaces* **4** 1600326
[155] Reynwar B J and Deserno M 2011 Membrane-mediated interactions between circular particles in the strongly curved regime *Soft Matter* **7** 8567
[156] Schweitzer Y and Kozlov M M 2015 Membrane-mediated interaction between strongly anisotropic protein scaffolds *PLoS Comput. Biol.* **11** e1004054
[157] Hu J, Lipowsky R and Weikl T R 2013 Binding constants of membrane-anchored receptors and ligands depend strongly on the nanoscale roughness of membranes *Proc. Natl Acad. Sci. USA* **110** 15283
[158] Xiong K, Zhao J, Yang D, Cheng Q, Wang J and Hi H 2017 Cooperative wrapping of nanoparticles of various sizes and shapes by lipid membranes *Soft Matter* **13** 4644